

AN IDEALISED STUDY OF THE STABILISATION MECHANISM IN THE LONG-TERM EVOLUTION OF CRESCENTIC BARS

Wen L. Chen¹, Nicholas Dodd¹ and Meinard C.H. Tiessen²

Abstract

The stabilisation mechanism in the long-term evolution of crescentic bars is investigated in this study. The model is an extended model of the model of Chen et al. (2017), built on linear stability analysis. The present model includes the effect of suppression of non-dominant lengthscales in addition to the nonlinear effects considered by Chen et al. (2017). With this model, the bathymetric evolution of crescentic bars at Duck (North Carolina, USA) for over 2 months period was reproduced. Results show that the suppression of non-dominant modes stabilizes the sea bed profile by sustaining the dominance of one morphological pattern and limiting the overall amplitude of the sea bed. The suppression effect can also influence the evolution of the dominant lengthscale. The threshold amplitude at which the suppression effect occurs selects the dominant lengthscale for the late post-storm stage. This study provides an alternative way in predicting the long-term evolution of crescentic systems.

Key words: crescentic bars, stabilisation, suppression effect, field observations

1. Introduction

Crescentic bars are a common morphological pattern in the nearshore region. They have been observed throughout the world (Van Enckevort et al., 2004). Such nearshore sea bed patterns are important in preventing coastal erosion and flooding (Hanley et al., 2014). However, due to the complexity of nearshore hydro- and morphodynamic, the mechanisms of long-term evolution of crescentic bar systems remain unclear.

Recently, the origin of crescentic bars has been shown in several studies to be due to morphological instability (see Ribas et al., 2015), owing to the positive feedback between developing topography and flow. Such instability in the sea bed is examined in many studies using linear stability analysis, see e.g. Deigaard et al. (1999); Falqués et al. (2000); Damgaard et al. (2002); Calvete et al. (2005); Van Leeuwen et al. (2006); Calvete et al. (2007). In this method, a perturbation of small amplitude can be imposed onto an equilibrium state. The interaction of flow and this perturbation results in a growth rate for this pattern. The pattern with largest growth rate will eventually dominate the sea bed profile. Although linear stability analysis has proved to be useful in describing the initialization and short term evolution of crescentic bars and identifying underlying physics (Van Enckevort et al. 2004), its performance in long-term prediction of crescentic bar evolution turns out to be less good (Tiessen et al., 2010). The limitation is due to the lack of nonlinear effects in linear stability analysis.

A few nonlinear effects are suggested to be important in the long-term evolution of crescentic bars by Tiessen et al. (2011). With a fully nonlinear numerical model, Tiessen et al. (2011) studied the impact of pre-existing bed-patterns and found a connection between the lengthscale of the pre-existing bed pattern and newly-arising crescentic bed-forms. A rapid initial development is found on higher harmonics of pre-existing lengthscale. Based on the work of Tiessen et al. (2011) work, Chen et al. (2017) identified the finite amplitude growth (equilibration) and higher harmonic interaction as the leading nonlinear effects in

1 Faculty of Engineering, University of Nottingham, University park, Nottingham, NG7 2RD, United Kingdom, wenlong.chen@nottingham.ac.uk.

2 Deltares, Marine and Coastal Systems Unit, Department of Environmental Hydrodynamics, Rotterdamseweg 185, 2629 HD Delft, The Netherlands.

the long-term development of crescentic bars. These effects are added to a linear stability model and used to predict crescentic bar evolution along a beach in Duck, North Carolina (USA). The predicted lengthscale of the dominant crescentic bar well reproduced the field observations. However, in the late post-storm stage, the predicted lengthscale shows some shifting instead of stabilisation on a main lengthscale, and the overall sea bed variance is over predicted.

Furthermore, the nonlinear numerical study of Smit et al. (2012) suggests a stable 2D morphology in the late post-storm stage. A bed pattern with significant amplitude is likely to remain until being removed by a storm, which means in the late post-storm stage the sea bed profile is stable and characterized with a dominant bed pattern. This is in agreement with field observations (Van Enckevort et al., 2004). Van Enckevort et al. (2004) found both splitting of the longest lengthscales and merging of small lengthscales in the late post-storm stage, which indicates a self-organization of crescentic bar system into a more uniform spacing and the suppression of non-dominant patterns. Such splitting and merging phenomena are also observed in numerical studies (Castelle and Ruessink, 2011).

In this study, we aim to investigate the stabilisation mechanism in the long-term evolution of crescentic bars in an idealised scheme, based on the work of Chen et al. (2017) and the conclusion of Smit et al. (2012).

To this end, the model of Chen et al. (2017) is extended to incorporate the suppression effect of non-dominant bed patterns, as suggested by Smit et al. (2012). The model is used to predict the lengthscale of the crescentic bed forms for a period of two months in 1998 at Duck (NC, USA). Measured wave conditions, tidal data and topography at the same field are used in the study. The model results are compared with field observation (Van Enckevort et al., 2004) over the same period.

The methodology used in this study is described in Section 2; Section 3 presents the results. Subsequently, the work is discussed in Section 4 and a conclusion is given in the final section.

2. METHODOLOGY

2.1 Model description

The model used here is based on the linear stability model of Calvete et al. (2005) (Morfo60). The framework of the model is composed of wave- and depth-averaged shallow water equations, complemented by wave energy and phase equations and a bed evolution equation. The model geometry describes an open coast of unlimited extent in the longshore direction. The quasi-steady assumption is adopted with a spatial coordinate system, (x,y) , aligned with cross- and long-shore directions respectively. Here, t refers to the morphodynamic time scale. Standard expressions are adopted for wave radiation stress, turbulent Reynolds stress, phase speed, group velocity, intrinsic and absolute frequency and wave orbital velocity (see Mei, 1989). Wave energy dissipation due to wave breaking is described according to Church and Thornton (1993). The expression of Feddersen et al. (2000) is used to describe the bed shear stress. Sediment transport follows the formulation of Soulsby and Van Rijn (Soulsby, 1997), which is a total load formula for combined transport by waves and currents. For full equations please see Calvete et al. (2005).

As in Chen et al. (2017), the initial bed and associated hydrodynamics under a set of forcing conditions (wave and water level) are obtained using Morfo60. To study the long-term evolution, non-linear effects have to be included. In addition to the equilibration and higher harmonic interaction, as adopted in Chen et al. (2017), here the suppression of non-dominant bed patterns is also accounted for.

2.2. Linear stability analysis

The variables of a standard linear stability analysis consist of a time invariant equilibrium state, plus a small perturbation to that state. In our study, the equilibrium state (so called basic state) corresponds to the prevailing wave condition and water levels throughout the 2 months at Duck (NC, USA). The wave data were recorded from August 20, 1998 until October 22, 1998 (Van Enckevort et al., 2004), at three hour intervals. So the alongshore-averaged topography was interpolated from the measurement (recorded

monthly) for all cross shore locations at the same frequency. The reproduced topography also incorporated tidal variation by shifting the water depth vertically. For complete information of wave conditions and water depths, please see Chen et al. (2017).

Once the basic state is obtained, a small perturbation is introduced onto the equilibrium state and the model equations are linearized with respect to that perturbation.

$$h' = \text{Re}\{h(x)e^{\omega t +iky}\}. \quad (1)$$

Here, h' represents the bed perturbation and $h(x)$ is its cross-shore profile, with arbitrary wavelength $\lambda = 2\pi/k$, and (complex) frequency $\omega = \omega_r + i\omega_i$. Thus the real part of the frequency ω_r represents the growth rate of the periodic pattern, while the imaginary part $c_m = \omega_i/k$ represents the corresponding migration rate. A pattern with positive (negative) ω_r indicates a growing (decaying) pattern. For a chosen k the cross-shore structure of the perturbation ($h(x)$) and its frequency (ω) are obtained using Morfo60 (Calvete et al. 2005).

2.3. Growth rate curve

The morphodynamic lengthscales observed in the field ranged from $k=0.001 \text{ rad m}^{-1}$ to $k=0.1 \text{ rad m}^{-1}$. We therefore calculated growth rate of these lengthscales in this range for increments $\Delta k = 0.001 \text{ rad m}^{-1}$, corresponding to λ values of {6.3km, 3.1km, 2.1km, 1.6km, 1.3km . . . 65.4m, 64.8m, 64.1m, 63.5m, 62.8m}, for each set of forcing conditions (every three hours, see section 2.2). To describe the amplitude development of all lengthscales, a unique growth rate (so-called physical growth rate) for each k is calculated for each three-hour prediction. The identification of an entire physical growth rate curve (in k space) is explained in Chen et al. (2017). An example of physical growth rate curve generated based on the condition on 20 August is shown in figure 1a.

The determination of the linear growth rate curve is done every three hours, based on the updated hydrodynamic forcing conditions and bathymetry. The variation of these growth rate curves over time is significant (see figure 1b) due to changes in wave forcing and tidal fluctuations.

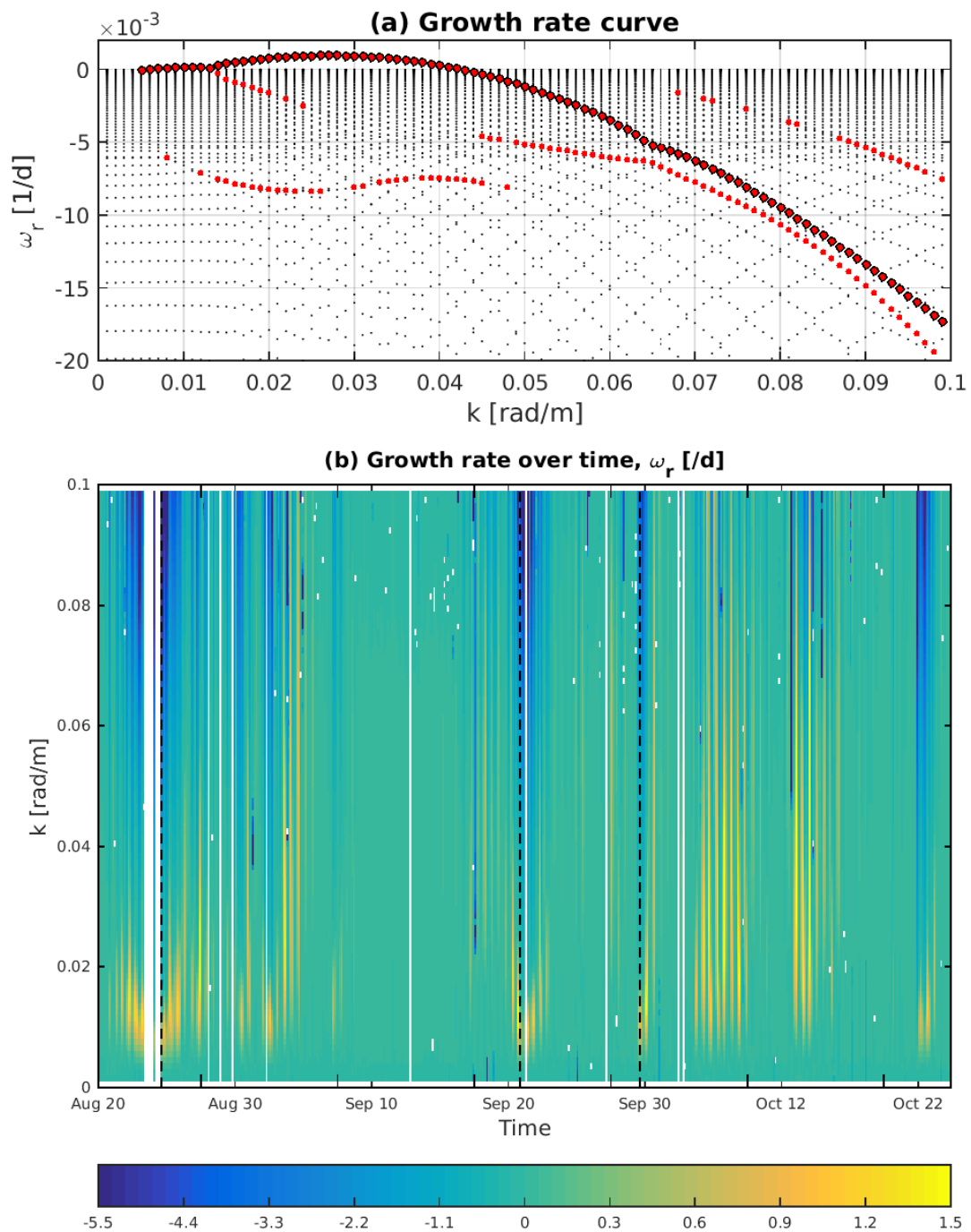


Figure 1. (a) Growth rate curve on August 20, 1998, with small black dots for all solutions from Morfo60, red dots for all physical modes and black encircled red dots for selected physical mode, covering k -value ranges from 0.001 to 0.1 rad m^{-1} ; (b) the growth rate curve at each time step (every three hours) as derived by selecting the most likely physical mode. Blue color indicates negative growth rate and yellow color indicates positive growth rate, and the black dashed line indicates the time of the peak of a storm.

2.4. Amplitude development

In linear stability theory, the amplitude of the perturbation follows an exponentially growing or decaying

evolution, which will violate the assumption of small perturbation after certain time of evolution. To study the long-term evolution, we thus need to incorporate non-linear effects. In this study, apart from non-linear effects adopted in Chen et al. (2017), i.e. equilibration and higher harmonic interactions, we also consider the suppression of all other modes when one pattern reaches a threshold of dominance. These effects are included in the amplitude equation below.

$$\frac{dA_\lambda}{dt} = \underbrace{\omega_{r\lambda}(t_n)A_\lambda}_I - \underbrace{l_\lambda(t_n)A_\lambda^3}_{II} + \underbrace{m_{2\lambda}A_{2\lambda}^2}_{III} - \underbrace{n_\lambda \left(0.5 + 0.5 \tanh \left(30(A_{\lambda_d} - A_{supp}) \right) \right)}_{IV}, \quad (2)$$

with

$$A_{min} = 0.1, A_{max} = 1, A_{supp} = 0.9, l_\lambda(t_n) = |\omega_\lambda|(t_n), m_{2\lambda} = \alpha(1 - A_\lambda^{10}), \alpha = 0.3.$$

and

$$\begin{aligned} n_\lambda &= 0.2, & \text{if } \lambda &\neq \lambda_d, \\ n_\lambda &= 0, & \text{if } \lambda &= \lambda_d. \end{aligned}$$

Note that $A_\lambda = A_\lambda(t_n)$ denotes the amplitude of the mode (bed pattern) of lengthscale λ at time t . Similarly $\omega_{r\lambda}(t_n)$ refers to the linear growth rate of lengthscale λ that pertains for $t_n \leq t < t_{n+1}$. The dominant lengthscale is denoted as λ_d , the amplitude of which (A_{λ_d}) is maximum of all lengthscales at that time. $A_\lambda(t = 0) = 0.1$ is the same for all lengthscales; as noted above, this is also the minimum amplitude. During storm events, all pre-existing bed-forms are expected to be erased. This is simulated by resetting the amplitudes of all lengthscales to $A_\lambda(t = 0)$. The maximum amplitude was set to 1. The values of A_{min} and A_{max} do not convey any significant meaning, except that a ten-fold growth seems to represent roughly the duration it takes for a crescentic bathymetry to reach a new stable situation after a storm.

On the right hand side, the first term (*I*) describes an initially exponentially growing (decaying) amplitude, assuming a small enough initial amplitude, with growth rate $\omega_{r\lambda}$. This is combined with a self-limiting term (*II*) to represent limiting finite-amplitude effects when bed-forms start to reach their final height. The form chosen is motivated by the Stuart-Landau equation (Drazin and Reid, 1981), which we refer to here as a Landau equation. The value of $l_\lambda(t_n)$ is chosen to ensure stabilisation of the bed-pattern amplitude when $|A_\lambda| \rightarrow 1$. Furthermore, an additional term representing the higher harmonic interaction (*III*) is implemented. This term allows the energy transfer to lengthscales that are half the original lengthscale, when this original lengthscale exhibits considerable amplitude itself. The energy transfer factor, $\alpha = 0.3$, was chosen (see Chen et al., 2017). The dependence of $m_{2\lambda}$ on A_λ is included to ensure that all modes can only achieve the same maximum amplitude, so that this term, if operational, accelerates growth only, and becomes inoperational as $|A_\lambda| \rightarrow 1$.

As mentioned earlier, the effect of equilibration (*II*) and higher harmonic interaction (*III*) were included in the model of Chen et al. (2017). To study the effect of suppression term of non-dominant modes, we introduce a fourth term (*IV*) into the amplitude development equation. Based on the amplitude development in the field, we use the formulation shown in equation (2), where A_{supp} refers to an amplitude when the suppression term is at ‘‘half strength’’. Here a value of 0.9 is chosen for A_{supp} , which means that if a dominant lengthscale attains an amplitude roughly between $0.85 < A_{\lambda_d} < 0.95$, the suppression of the other lengthscales occurs. Note that the factor 30 in term IV means that this term is activated/de-activated fairly abruptly at this threshold. The level of suppression is governed by n_λ .

3. RESULTS

The model is used to study the evolution of crescentic bars at Duck for a period of two months, from 20 August 1998 until 22 October 1998. The forcing and geometry used in this study are observations at the same field (Van Enkevort et al., 2004), as mentioned in section 2.2. The predicted amplitude development for all examined lengthscales is shown over time in figure 2. Scenarios with and without the suppression effect are presented in figure 2a and 2b, respectively, with light color indicating low amplitude and dark color high amplitude. In all early post storm stages, figure 2a and 2b show the same amplitude development. Only after a certain time of evolution, the suppression term in figure 2a appears to be

effective after both storm 1 and 3. This is as expected, since the suppression term only works when the amplitude of one mode (dominant lengthscale) reaches a certain value. The non-dominant lengthscales are eradicated afterwards. Note that the suppression term is not activated after storm 2, this is because the interval between storm 2 and 3 is not long enough for the amplitude of any length scale to reach the threshold amplitude.

A comparison with the field observations of Van Enkevort et al. (2004) is also shown in figure 2. The predicted dominant lengthscale (the biggest amplitude at each time $t = t_n$) is shown as a coloured dot, and the observed lengthscales are shown as larger white dots. The effect of the suppression term in figure 2a results in the rapid disappearance of any lengthscale other than the dominant mode. For the post-storm-1 period, this occurs approximately at the same time as when the dominant lengthscale in figure 2b drops below the observed lengthscale (4 September). The suppression term, therefore, results in the stabilisation of the bathymetry and the ongoing dominance of a lengthscale that lies reasonably close to the observed lengthscale. After the third storm, a similar behaviour is observed at about 10 October. However, observation after the third storm shows continued fluctuation of lengthscale (see Fig. 2a), allied to a more narrowed band compared to the immediate post-storm period.

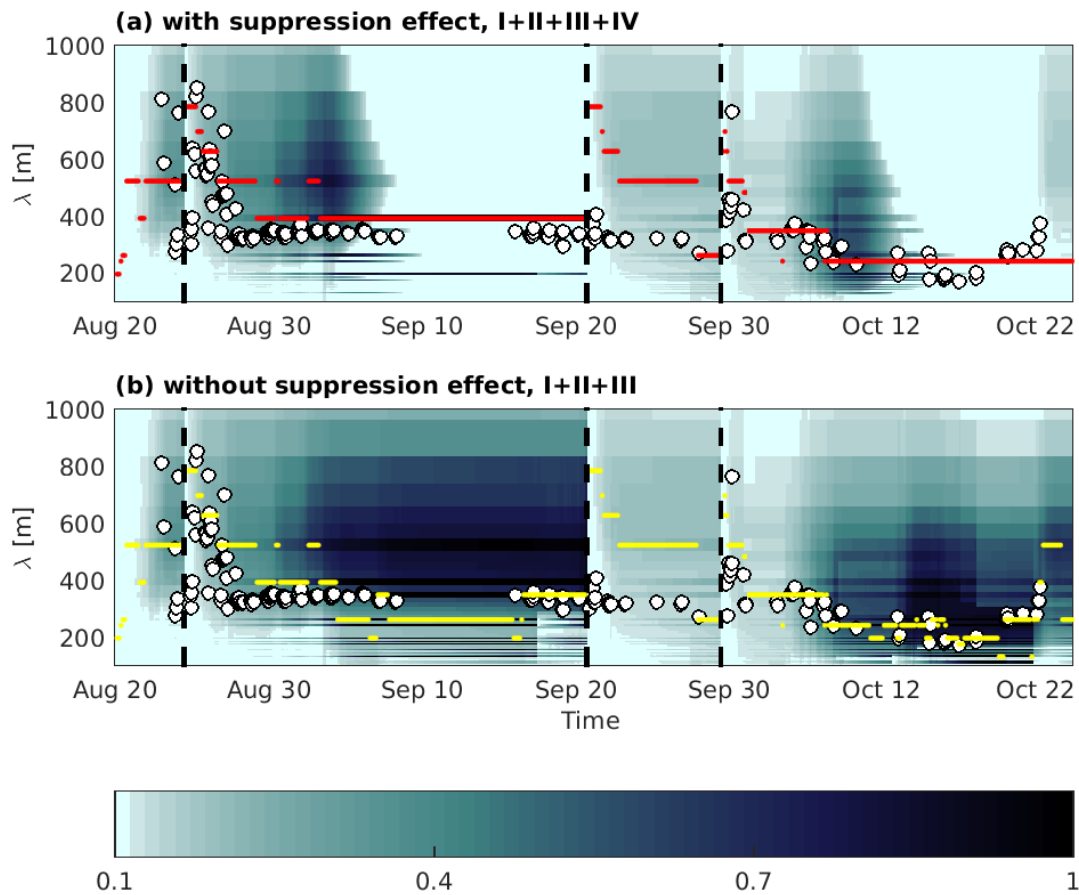


Figure 2. Amplitude development for scenario (a) with suppression effect, $I+II+III+IV$; and (b) without suppression effect, $I+II+III$. The predicted dominant lengthscales are labeled with coloured dots, and observed lengthscales, according to Van Enkevort et al. (2004), are illustrated as large white circles.

4. Discussion

A quantitative comparison between the observed and predicted lengthscale shows that the inclusion of suppression effect appears to be unimportant for the prediction of dominant lengthscale. In the scenario

without suppression effect, model produces a relative error of 0.31. With the suppression effect, model produces a similar relative error, 0.33. Note that the comparison is taken at the moments when observation could be made, and the relative errors are averaged values. Though the suppression term shows no improvement in predicting the dominant length scale, it is important when considering the evolution and stabilisation of the whole bed profile. As shown in Fig. 3, with the aid of the suppression effect, the averaged amplitude, $\bar{A}(t_n) = \frac{1}{N_\lambda} \sum_{j=1}^{N_\lambda} A_j(t_n)$, of model prediction is smaller than that of without suppression effect. Note the additional suppression term is only effective for the later post-storm periods when shorter lengthscales are dominant, which is in line with the finding of Smit et al. (2012).

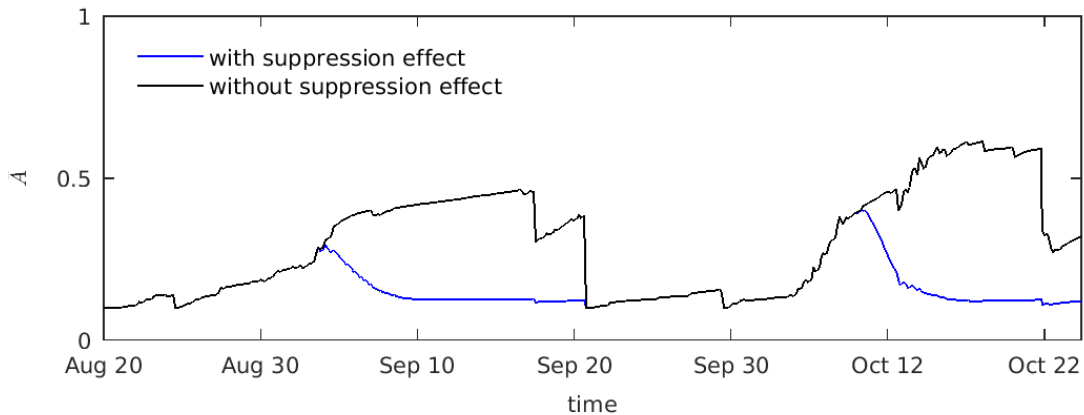


Figure 3. Averaged amplitude (\bar{A}) over time, with blue and black solid for scenario with and without suppression effect, respectively.

In this study, the threshold amplitude when the suppression effect occurs is defined by parameter A_{supp} . Here, a value of 0.9 is chosen, which means the suppression effect occurs when the amplitude of dominant lengthscale reaches around 0.85. This value is estimated based on observations (Van Enckevort et al., 2004). There is no specific study on this threshold amplitude yet. Smit et al. (2012) did look into the effect of force duration (which also means the development duration of preferred bed pattern) on the stability of sea bed, but no effort is given on the amplitude. The sensitivity of relative error between predicted and observed lengthscale on the value of A_{supp} is examined and shown in figure 4. By allowing A_{supp} to gradually increase from 0.6 to 1, the relative error first stays at around 0.32 then experiences a sudden increase to 0.4 when A_{supp} is around 0.72. This is because the selected dominant lengthscale changes for various A_{supp} . To illustrate this, the amplitude evolutions for $A_{supp} = 0.65$ (pink dot in figure 4), $A_{supp} = 0.75$ (blue dot) and $A_{supp} = 0.9$ (red dot) are presented in figure 5. In figure 5a, the suppression effect occurs at around 30 August, leading to a dominant lengthscale around 400 m which is quite close to the observation, the predicted dominant lengthscale stays at this value afterwards because of the suppression effect. On the other hand, in figure 5b, the suppression effect occurs at around 2 September, with a dominant lengthscale close to 550 m. The suppression effect opposes the higher harmonic interaction, thus preventing the energy to be transferred from 550 m lengthscale to shorter lengthscales, resulting in a big relative error between observed and predicted lengthscales. For $A_{supp} = 0.9$, also the value used in this study, the suppression effect occurs at around 4 September when the dominant lengthscale is at 400m. The threshold amplitude is important for the stabilisation of crescentic bars and the evolution of crescentic bars. More studies are required for the determination of this parameter.

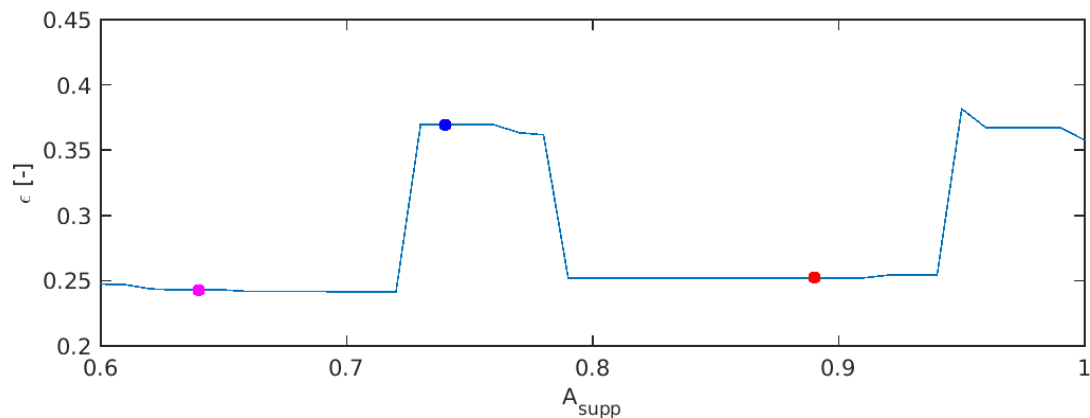


Figure 4. Sensitivity of relative error between predicted and observed lengthscales on A_{supp} .

5. Conclusion

In this study, we investigated the stabilisation mechanism in the long-term evolution of crescentic bar systems. The model of Chen et al. (2017) is extended by including the suppression effect of non-dominant lengthscales in the amplitude development equation. Using the new model, the bathymetric evolution of crescentic-barred beaches at Duck (NC) from 20 August to 22 October 1998 was reproduced. The field observations, i.e., wave conditions, water levels and crescentic bar information, over the same period were obtained from Van Enkevort et al. (2004).

Results show that the inclusion of the suppression effect of the non-dominant lengthscales leads to the stabilisation of sea bed, by limiting the overall amplitude of bathymetry and sustaining the dominance of a few lengthscales in later post-storm stage. The suppression effect can also affect the evolution of the dominant lengthscales. The threshold amplitude determines the moment when the suppression effect starts working, and hence determines the dominant lengthscales.

Overall, implementing the nonlinear effects identified in Chen et al. (2017), i.e., damping of amplitude growth and the transfer of energy to higher harmonic lengthscales, together with the suppression of non-dominant lengthscales, into a linear stability model can well describe the nonlinear evolution of a crescentic bar system. Moreover, the model investigated in this study requires limited bathymetric data and performs with high computational efficiency. This study thus provides an alternative way other than use of a complicated numerical model in predicting long-term morphological development of crescentic bars and identifying the underlying physics.

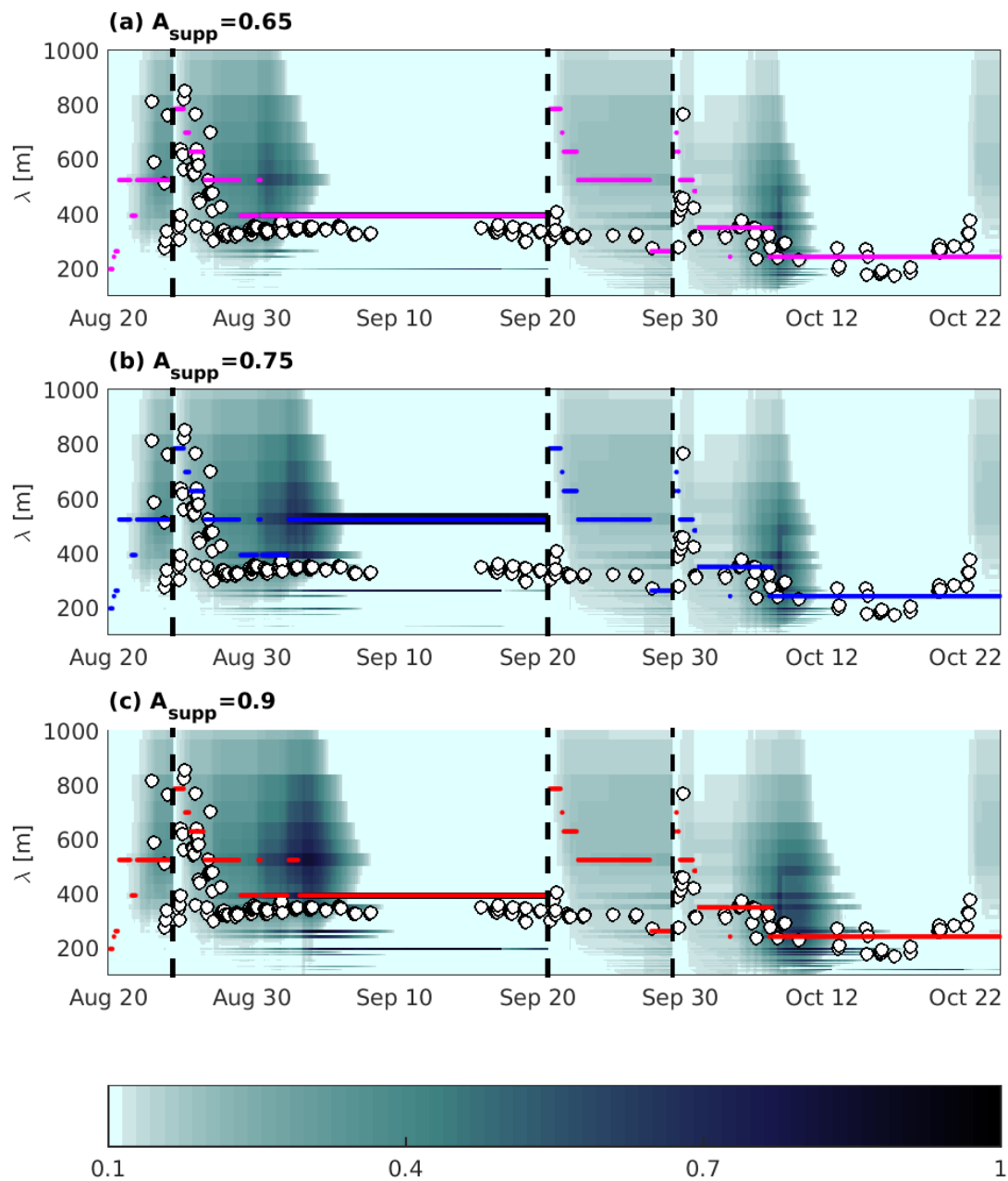


Figure 5. Amplitude development for (a) $A_{supp} = 0.65$; (b) $A_{supp} = 0.75$; and (c) $A_{supp} = 0.9$.

Acknowledgements

The support of the UK Engineering and Physical Sciences Research Council (EPSRC) under the MORPHINE project (grant EP/N007379/1) and of the University of Nottingham is gratefully acknowledged.

References

Calvete, D., Dodd, N., Falqués, A. and Van Leeuwen, S. M., 2005. Morphological development of rip channel systems: normal and near normal wave incidence, *J. Geophys. Res.*, 110 (C10), C10,007.

- Calvete, D., Coco, G., Falqués, A. and Dodd, N. 2007. (un)predictability in rip channel systems, *Geophys. Res. Lett.*, 34 (L05605).
- Church, J. C., and Thornton, E. B., 1993. Effects of breaking of the longshore current, *Coastal Eng.*, 20, 1–28.
- Chen, W. L., Dodd, N., Tiessen, M. C. H. and Calvete, D., 2017. An idealised study for the long term evolution of crescentic bars. Submitted.
- Castelle, B., and Ruessink, B. G., 2011. Modelling formation and subsequent nonlinear evolution of rip channels: Time varying versus timeinvariant wave forcing, *J. Geophys. Res.*, 116, F04008.
- Damgaard, J. S., Dodd, N., Hall, L. J. and Chesher, T. J., 2002. Morphodynamic modelling of rip channel growth, *Coastal Eng.*, 45, 199–221.
- Deigaard, R., Drønen, R., Fredsøe, J. Jensen, J. H. and Jørgensen, M. P., 1999. A morphological stability analysis for a long straight barred beach, *Coastal Eng.*, 36(3), 171–195.
- Dodd, N., Blondeaux, P., Calvete, D., de Swart, H.E., Falques, A., Hulscher, S. J., Rozynski, G. and Vittori, G., 2003. Understanding coastal morphodynamics using stability methods, *Journal of coastal research*, 19 (4), 849–865.
- Drazin, P. G., and Reid, W. H., 1981. *Hydrodynamic Stability*, 527 pp., Cambridge Univ. Press, New York.
- Falqués, A., Coco, G. and Huntley, D. A., 2000. A mechanism for the generation of wave driven rhythmic patterns in the surf zone, *J. Geophys. Res.*, 105 (C10), 24,071–24,087.
- Fedderson, F., Guza, R. T. and Elgar, S., 2000. Velocity moments in alongshore bottom stress parameterizations, *J. Geophys. Res.*, 105(C4), 8673–8686.
- Hanley, M., Hogart, S., Simmonds, D., Bichot, A., Colangelo, M., Bozzeda, F., Heurtefeux, H., Ondiviela, B., Ostrowski, R., Recio, M., Trude, R., Zawadzka-Kahlau, E. and Thompson, R., 2014. Shifting sands? coastal protection by sand banks, beaches and dunes, *Coastal Engineering*, 87 (0), 136 – 146.
- Mei, C. C., 1989. *The applied dynamics of ocean surface waves*. World scientific, Singapore.
- Ribas, F., Falqués, A., de Swart, H. E., Dodd, N., Garnier, R. and Calvete, D., 2015. Understanding coastal morphodynamic patterns from depth-averaged sediment concentration, *Rev. Geophys.*, 53 (2), 362–410.
- Schielen, R., Doelman, A. and de Swart, H. E., 1993. On the dynamics of free bars in straight channels, *J. Fluid Mech.*, 252, 325–356.
- Smit, M. Reniers, W. J., A. J. H. M. and Stive, M. J. F., 2012. Role of morphological variability in the evolution of nearshore sandbars, *Coastal Eng.*, 69, 19–28.
- Soulsby, R. L., 1997. *Dynamics of Marine Sands*, 249 pp., Thomas Telford, London.
- Tiessen, M. C. H., van Leeuwen, S. M., Calvete, D. and Dodd, N., 2010. A field test of a linear stability model for crescentic bars, *Coastal Eng.*, 57 , 41–51.
- Tiessen, M. C. H., Dodd, N. and Garnier, R., 2011. Development of crescentic bars for a periodically perturbed initial bathymetry, *J. Geophys. Res.*, 116, F04,016.
- Van Enckevort, I. M. J., Ruessink, B. G., Coco, G., Suzukui, K., Turner, I. L., Plant, N. G. and Holman, R. A., 2004. Observations of nearshore crescentic sandbars, *J. Geophys. Res.*, 109 (C06028).
- Van Leeuwen, S. M., Dodd, N., Calvete, D. and Falqués, A., 2006. Physics of nearshore bed pattern formation under regular or random waves, *J. Geophys. Res.*, 111 (F01023).